tvst

Glaucoma

# Effect of Strain on Rodent Glaucoma Models: Magnetic Bead Injection Versus Hydrogel Injection Versus Circumlimbal Suture

**Kyoung Min Lee[1,2], Da Young Song[2], and Seok Hwan Kim[1,2]**

[1] Department of Ophthalmology, Seoul National University College of Medicine, Seoul, Korea
[2] Department of Ophthalmology, Seoul National University Boramae Medical Center, Seoul, Korea

**Correspondence:** Seok Hwan Kim, Department of Ophthalmology, Seoul National University Boramae Medical Center, 39 Boramae Road, Dongjak-gu, Seoul 07061, Korea.
e-mail: xcski@hanmail.net

**Received:** May 11, 2022
**Accepted:** September 14, 2022
**Published:** September 29, 2022

**Keywords:** glaucoma animal model; magnetic bead injection; hydrogel injection; circumlimbal suture; rat strain

**Citation:** Lee KM, Song DY, Kim SH. Effect of strain on rodent glaucoma models: Magnetic bead injection versus hydrogel injection versus circumlimbal suture. Transl Vis Sci Technol. 2022;11(9):31, https://doi.org/10.1167/tvst.11.9.31

**Purpose:** To compare the inter-strain differences of three rodent glaucoma models as induced by magnetic bead injection, hydrogel injection, and circumlimbal suture.

**Methods:** In Brown Norway (BN) and Sprague Dawley (SD) rat strains, intraocular pressure (IOP) was elevated by injection of magnetic beads or hydrogel to obstruct the aqueous humor outflow or by external compression of circumlimbal suture. Maximum and average IOP values were compared according to both procedure and rat strain over 1 month postoperatively. Retinal ganglion cell (RGC) density loss was evaluated using confocal microscopic images of the flat-mounted retina obtained at postoperative days 14 and 30.

**Results:** The maximum IOPs were higher in the hydrogel injection or circumlimbal injection models than in the magnetic bead injection model ($P < 0.001$), whereas average IOP showed no difference between the two strains (both $P \geq 0.05$). A generalized estimating equation regression model showed that the IOP increase was maintained better in the BN rats than in the SD rats ($P < 0.001$). Such inter-strain difference was smaller in the circumlimbal suture model. A significant decrease in RGC density was observed in all of the models for the BN rats and in the circumlimbal suture model for the SD rats at postoperative day 30.

**Conclusions:** BN rats were advantageous for the magnetic bead or hydrogel injection model, but either rat strain could be used for the circumlimbal suture model. Strains should be considered cautiously when establishing rodent glaucoma models with different IOP profiles.

**Translational Relevance:** This comparison offers the best strain for each rodent glaucoma model for assessment of glaucoma-relevant therapeutics.

## Introduction

Glaucoma is the leading cause of irreversible blindness in the world,[1] and its prevalence is expected to increase steadily.[2,3] The characteristic feature of glaucoma is progressive axonal loss of retinal ganglion cells (RGCs), but its detailed pathophysiology has yet to be fully explained.[4] Many factors such as mechanical, ischemic, metabolic, and immunologic insults have been nominated as candidate sources of axonal damage[4–7]; however, intraocular pressure (IOP) is the only controllable factor in practice.

To understand the pathogenesis of glaucoma and to improve its therapy, various glaucoma animal models have been developed in many species, including monkeys,[8–11] dogs,[12] and rodents (mice/rats).[13–38] Those models were designed to have inducibly or spontaneously increased IOP. Among them, rodent glaucoma models are frequently used due to the ease and low cost of implementation. Most currently available rodent models are accomplished by laser treatment of the outflow area,[13–15] cautery or affliction of osmotic damage to the episcleral and vortex veins,[16,17] external ocular compression using circumlimbal suture,[18–20] or injection of beads[21–28] or hydrogel[33–38] into the anterior chamber.

Each rodent glaucoma model, however, is established based on a different rat strain,[28] and strains are reported to have different IOP and RGC death profiles.[22,26] Therefore, in order to improve the efficiency of any rodent glaucoma model, inter-strain comparison is necessary. The purpose of the present study was to compare three rodent glaucoma models—magnetic bead injection model, hydrogel injection model, and circumlimbal suture model—against two different rat strains: Brown Norway (BN) and Sprague Dawley (SD). This comparison will enable the use of the most effective strain for each model and thus facilitate better use of rodent glaucoma models for disease and treatment discovery and testing.

# Methods

## Animals

This study was conducted in accordance with the ARVO Statement for the Use of Animals in Ophthalmic and Visual Research, using protocols approved and monitored by the Seoul National University Boramae Medical Center Institutional Animal Care and Use Committee (no. 2021-0023). Eight-month-old male BN rats ($n$ = 70) and male SD rats ($n$ = 50), each weighing 250 to 300 g, were housed in a constant low-light environment (40–60 lux) to minimize diurnal fluctuations in IOP, with food and water provided ad libitum. All of the surgical procedures were performed under general anesthesia induced by isoflurane inhalation (Fig. 1).

## Measurement of IOP

IOP was measured three times preoperatively to calculate the baseline and was again measured immediately postoperatively and on postoperative day 1, postoperative day 2, and every 3 to 4 days up to 1 month after injection using a rebound tonometer (iCare TONOLAB tonometer; Tonovet, Vantaa, Finland) specifically calibrated for use with the rat eye.[39] All measurements were made in awake animals under topical anesthesia induced by 0.5% proparacaine hydrochloride eye drops (Hanmi Pharmaceutical Co., Seoul, Korea). IOP was measured five times for a single measurement. The mean of those values was calculated after excluding the highest and lowest results and subsequently used in the analysis. Besides individual IOP values, two representative values were also investigated: (1) maximum IOP value during

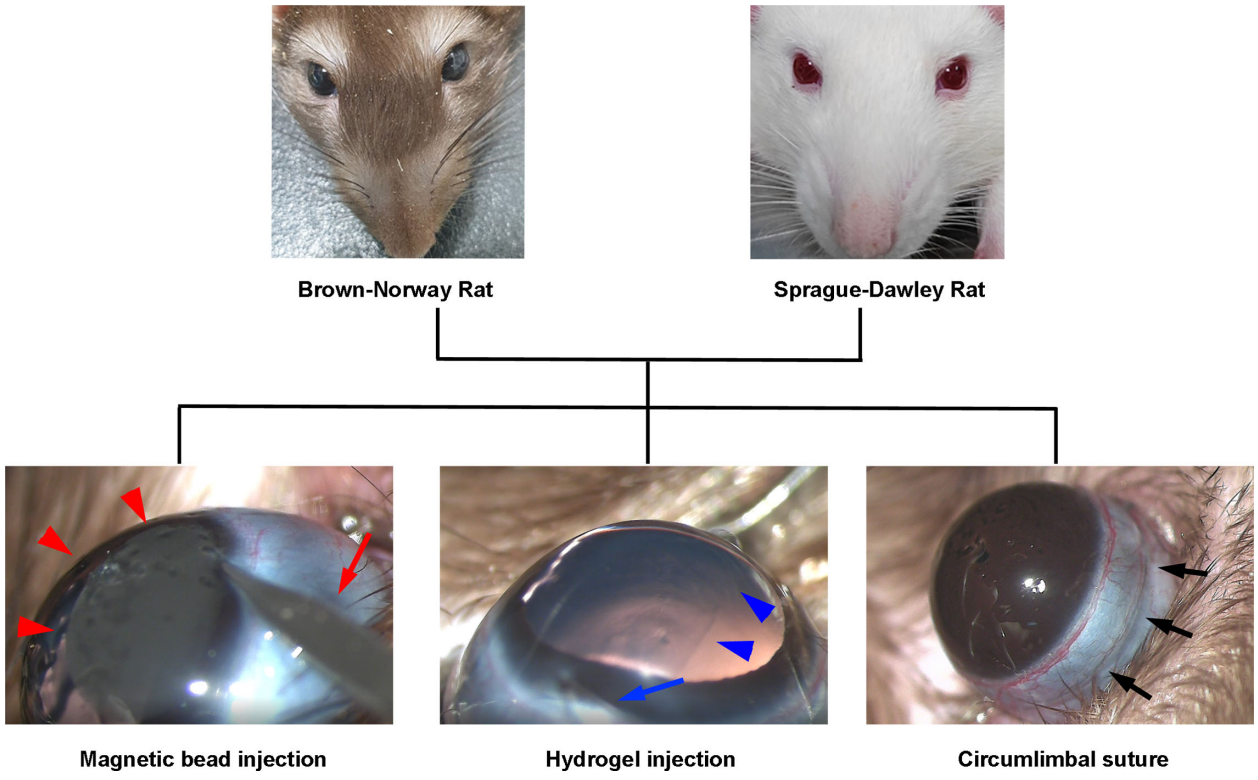


**Figure 1.** Study design scheme. Brown Norway and Sprague Dawley rats were compared for three rodent glaucoma models. Aqueous humor outflow was obstructed by injection of either magnetic beads (*red arrowheads*; Supplementary Movie S1) or hydrogel (*blue arrowheads*; Supplementary Movie S2). For this purpose, the glass capillary needle was fabricated to have very narrow and sharp tips (*red* and *blue arrows*). External pressure was applied by circumlimbal suture 1.0 to ~1.5 mm behind the limbus (*black arrows*; Supplementary Movie S3).

**Table 1.** Demographics and IOP Profiles of Each Group

| IOP Parameters | Magnetic Bead Injection (A) | Hydrogel Injection (B) | Circumlimbal Suture (C) | $P$[a] | Post Hoc Analysis |
|---|---|---|---|---|---|
| Brown Norway rat, *n* | 26 | 26 | 18 | — | |
| Baseline IOP (mmHg) | 12.8 ± 0.8 | 13.0 ± 1.2 | 13.1 ± 1.6 | 0.714 | |
| Maximum IOP (mmHg) | 34.3 ± 14.6 | 53.8 ± 15.8 | 54.3 ± 18.3 | <0.001 | A < B = C |
| Average integral IOP (mmHg) | 24.7 ± 8.5 | 27.0 ± 12.8 | 25.9 ± 10.5 | 0.782 | |
| Sprague Dawley rat, *n* | 17 | 17 | 16 | — | |
| Baseline IOP (mmHg) | 12.9 ± 0.9 | 12.7 ± 0.7 | 12.9 ± 0.9 | 0.828 | |
| Maximum IOP (mmHg) | 25.6 ± 9.5 | 50.7 ± 19.8 | 45.9 ± 14.5 | <0.001 | A < B = C |
| Average integral IOP (mmHg) | 16.3 ± 4.1 | 21.3 ± 12.0 | 25.7 ± 11.8 | 0.059 | |

[a]Comparison was performed using a one-way analysis of variance test with post hoc Scheffe analysis.

follow-up, and (2) average integral IOP, defined as the area under the IOP curve[38,40] divided by the observed days for each subject (Table 1).

## Induction of Ocular Hypertension

### Preparation of Injection Setup

A glass micropipette for ocular injection was made by pulling a glass capillary tube with a micropuller (PC-100; Narishige, Tokyo, Japan). One of the tips of the tube was broken and ground using a microgrinder (EG-401; Narishige). After filling the glass capillary tube with injection materials (magnetic bead or hydrogel), the tube was connected to a pneumatic microinjector (IM-11-2; Narishige) for application of positive continuous pressure to facilitate full delivery throughout the injection with no dead spaces.

### Magnetic Bead Injection

Twenty-six BN rats and 17 SD rats were subjected to magnetic bead injection. Magnetic beads were prepared at the concentration of 15 mg carboxyl ferromagnetic microspheres per milliliter, mixing intermediate size microspheres (diameter, 8.0–8.9 µm; CFM-80-5; Spherotech, Lake Forest, IL) with small size microspheres (diameter, 4.0–4.9 µm; CFM-40-10; Spherotech) at a 2:1 ratio.[41,42] The inside of the glass capillary tube was filled with 10 µL of magnetic bead solution using a Hamilton syringe. The empty space of the tube in the tail was filled with viscoelastic material (DisCoVisc; Alcon, Fort Worth, TX). In each procedure, the magnetic bead solution and viscoelastic material were injected into the anterior chamber through a tunnel located near and parallel to the limbus. After injection, a handheld magnet was applied to the side opposite the injection to prevent reflux spillage of magnetic beads through the incision tunnel (Fig. 1, Supplementary Movie S1).[25,29,32]

### Hydrogel Injection

Twenty-six BN rats and 17 SD rats were subjected to hydrogel injection. For this purpose, a premixed in situ cross-linking hydrogel (HyStem Cell Culture Scaffold [HCCS] kit; Sigma-Aldrich, St. Louis, MO) was injected into the anterior chamber in the same manner as reported previously.[34,37] The HCCS kit consisted of HyStem (thiol-modified carboxymethyl hyaluronic acid) and Extralink (thiol-reactive polyethylene glycol diacrylate), both dissolved in degassed water according to the manufacturer's instructions and mixed at a ratio of 4:1 immediately before injection.[34,37] The inside of the glass capillary tube was filled with 10 µL HCCS using a Hamilton syringe, as in the magnetic bead injection model. The empty space of the tube in the tail was filled with viscoelastic material (DisCoVisc), again consistent with the magnetic bead injection model. In each procedure, the HCCS and viscoelastic material were injected into the anterior chamber through a tunnel located near and parallel to the limbus (Fig. 1, Supplementary Movie S2).

### Circumlimbal Suture

Eighteen BN rats and 16 SD rats were subjected to circumlimbal suturing. The suturing was performed around the globe approximately 1.0 to 1.5 mm behind the limbus using 7/0 nylon to pressurize the eyeball as in previous reports (Fig. 1, Supplementary Movie S3).[18–20]

### RGC Counts

To determine the number of RGCs, the rats were heavily anesthetized on days 14 and 30 by isoflurane inhalation and euthanized in a $CO_2$ chamber, affording at least five samples for each time point of the glaucoma model. For comparison, five additional samples were obtained from healthy subjects for each strain. Eyes were immediately enucleated and fixed

with 10% neutral buffered formalin for 4 minutes at room temperature. After that, the retina was dissected and flattened with four radial cuts, the vitreous was removed, and the retina was flat-mounted, RGC layer up, on a glass slide. The retinas were labeled with RGC-targeting anti-Brn3a antibody (sc-8429; Santa Cruz Biotechnology, Dallas, TX) and counterstained with 4′,6-diamidino-2-phenylindole (D9542, Sigma-Aldrich). Then, the retinas, still flat-mounted, were imaged by confocal microscopy (STELLARIS 8; Leica, Wetzlar, Germany) for quantification of RGC densities. A total of 36 images for each eye (three spots for each 1-, 2-, and 3-mm area from the optic nerve head in four quadrants) were obtained (200 × magnification; 0.31 µm/pixel). RGCs were counted by the automated cell-counting software developed by Guymer et al.[43]

## Statistical Analysis

All statistical analyses were performed with commercially available software (Stata 16.0; StataCorp, College Station, TX) and R 4.1.2 (R Foundation for Statistical Computing, Vienna, Austria). A generalized estimating equation (GEE) regression model was applied to simulate the IOP change over time according to the glaucoma model and strain. RGC density was compared by Kruskal–Wallis testing. The data herein are presented as mean ± standard deviations except where stated otherwise; the cutoff for statistical significance was set to $P < 0.05$.

# Results

## IOP Elevation Profile

Following the surgical procedures, IOP increased and then slowly decreased with time in all cases (Fig. 2). The pattern of IOP increase, however, differed among the procedures. The magnetic bead injection model induced a gradual increase of IOP; the hydrogel injection model induced a spike immediately postopera-

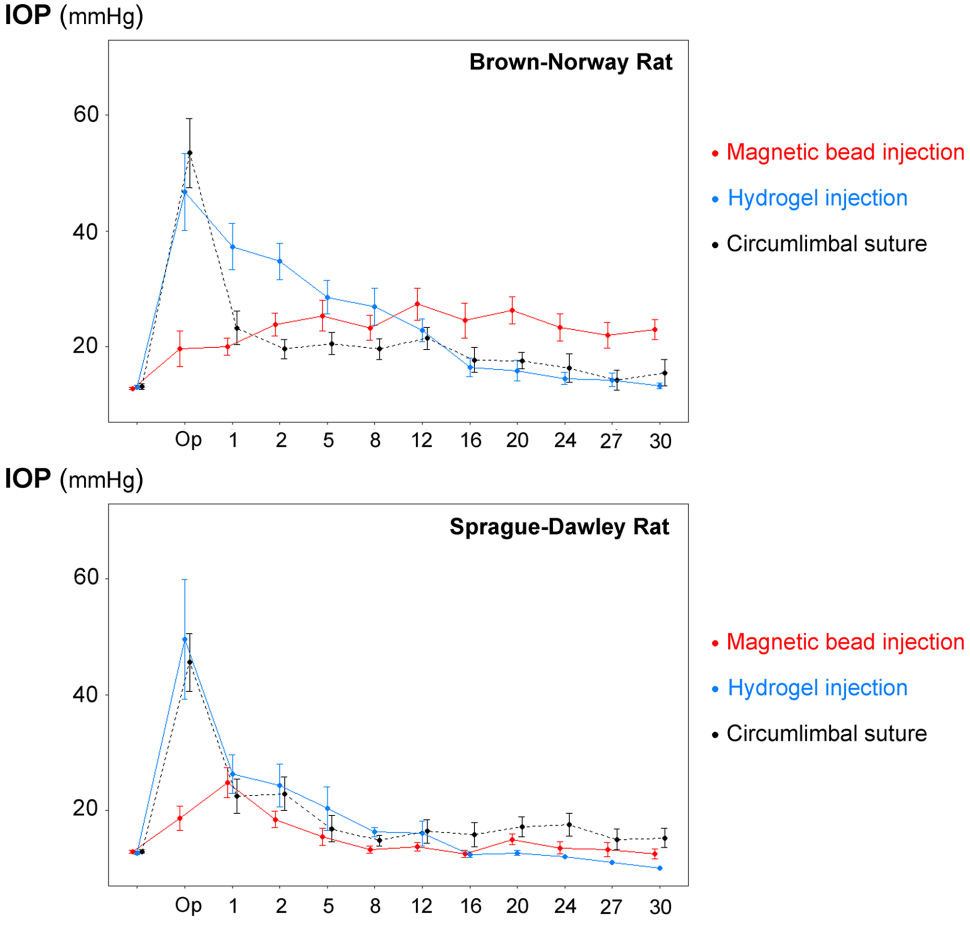


**Figure 2.** IOP profiles according to strains and rodent glaucoma models. The magnetic bead injection model induced a gradual increase in IOP. The hydrogel injection model induced an immediate IOP increase followed by a gradual decrease. The circumlimbal suture model induced an immediate IOP spike followed by a rapid decrease of IOP. The magnetic bead and hydrogel injection models maintained IOP increases longer in BN rats than in SD rats. *Bars* indicate 95% confidence intervals.

**Table 2.** IOP According to Postoperative Day, Glaucoma Animal Model, and Strain

| | Generalized Estimating Equation Regression Model | | | |
|---|---|---|---|---|
| | Coefficient | Standard Error | 95% Confidence Interval | *P* |
| Postoperative day | 0.069 | 0.036 | (−0.002, 0.140) | 0.056 |
| Glaucoma animal model (vs. magnetic bead injection) | | | | |
| Hydrogel injection | **13.406** | **0.847** | **(11.745, 15.067)** | **<0.001** |
| Circumlimbal suture | **13.658** | **0.771** | **(12.148, 15.169)** | **<0.001** |
| Strain (vs. Brown Norway rat) | | | | |
| Sprague Dawley rat | **−2.755** | **0.671** | **(−4.070, −1.439)** | **<0.001** |

Statistically significant values ($P < 0.05$) are shown in bold.

tively with a gradual decrease of IOP thereafter; and the circumlimbal suture model induced an immediately postoperative spike with rapid decrease of IOP thereafter (Fig. 2). The maximum IOP was higher in the hydrogel injection and circumlimbal suture models than in the magnetic bead injection model, whereas the average integral IOP showed no difference among the models (Table 1).

The constructed GEE regression model evaluated the effects of each procedure and strain on the IOP profile (Table 2). Increased IOP was slowly normalized as time passed. The hydrogel injection and the circumlimbal suture models induced more abrupt IOP increases (both $P < 0.001$) than did the magnetic bead injection model. The SD rat strain showed lesser IOP elevation ($P < 0.001$) than did the BN rat strain.

## Differences Among Glaucoma Models

Eye enlargement (buphthalmos) was observed in all of the BN rats in the magnetic bead injection model group (Figs. 3A$_1$, 3A2, red arrows), but in only four (15%) of the BN rats in the hydrogel injection model group (Fig. 3A$_3$, blue arrow) and one (6%) of the SD rats in the magnetic bead injection model group (Fig. 3A$_4$, orange arrow). Three of the 26

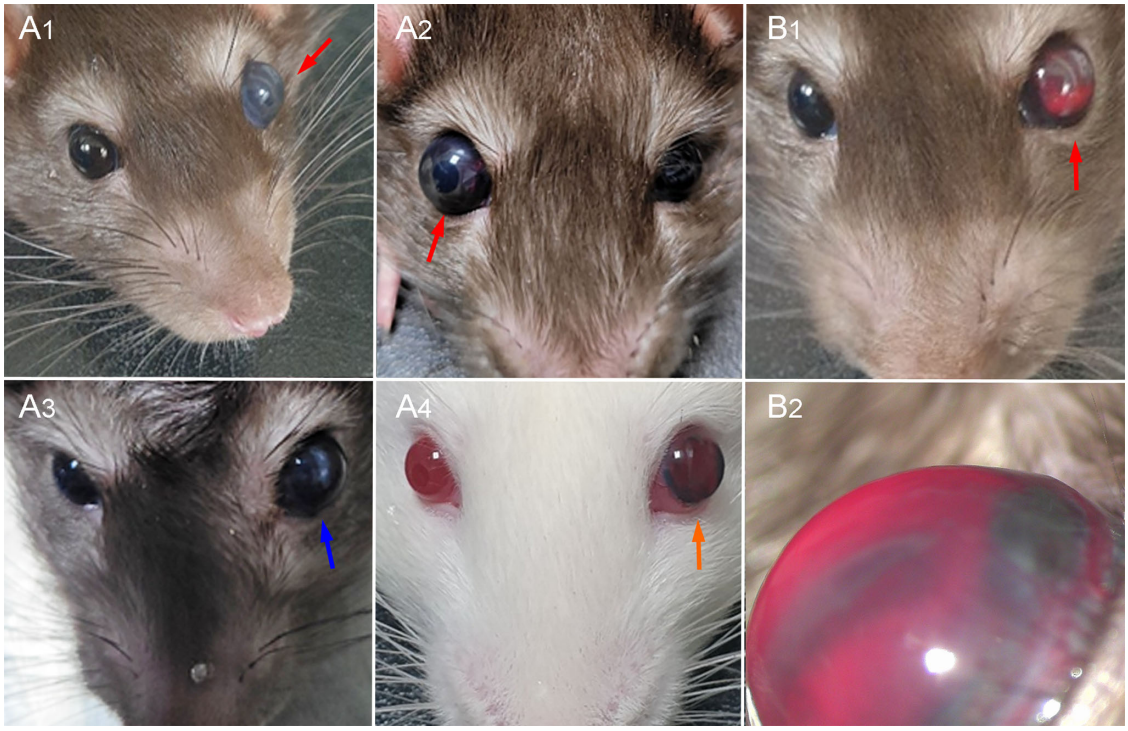


**Figure 3.** Gross anatomic changes. (A) Buphthalmos in the magnetic bead injection model of BN rats (A$_1$ and A$_2$, *red arrows*), in the hydrogel injection model of BN rats (A$_3$, *blue arrow*), and in the magnetic bead injection model of SD rats (A$_4$, *orange arrow*). These changes were not observed in the circumlimbal suture model. (B) Neovascular complications in the magnetic bead injection model (B$_1$, *red arrow*). These changes were not observed in the hydrogel injection model nor in the circumlimbal suture model.

**Table 3.** RGC Density Changes According to Glaucoma Animal Model and Strain

| Cell Counts/mm$^2$ | Magnetic Bead Injection | Hydrogel Injection | Circumlimbal Suture | *P* (Over Models) |
|---|---|---|---|---|
| Brown Norway rat (control) | | 1886 ± 456 | | |
| Day 14 | 1485 ± 418 | 1662 ± 479 | 1791 ± 506 | 0.011[a] |
| Day 30 | 1145 ± 506 | 1346 ± 688 | 1413 ± 519 | 0.304[a] |
| *P* (over weeks) | <0.001[a] | <0.001[a] | 0.028[a] | — |
| Sprague Dawley rat (control) | | 1872 ± 210 | | |
| Day 14 | 1703 ± 617 | 1706 ± 416 | 1734 ± 494 | 0.945[a] |
| Day 30 | 1694 ± 430 | 1683 ± 446 | 1456 ± 432 | 0.181[a] |
| *P* (over weeks) | 0.425[a] | 0.489[a] | <0.001[a] | — |

[a]Comparison was performed using Kruskal–Wallis test.

eyes (12%) among the magnetic-bead-injected BN rats developed hyphema as a consequence of neovascular complication and thus were excluded from the analysis (Figs. 3B$_1$, 3B2, red arrow). No neovascular complications were observed in either the hydrogel injection or circumlimbal suture model.

## RGC Comparison

For the BN rats, the average RGC density (cell counts/mm$^2$) was 1886 ± 456, which had decreased to 1485 ± 418 (78.7% ± 22.2%) at day 14 and 1145 ± 506 (60.7% ± 26.8%) at day 30 after magnetic bead injection ($P < 0.001$). After hydrogel injection, the RGC density decreased to 1662 ± 479 (88.1% ± 25.4%) at day 14 and 1346 ± 688 (71.4% ± 36.5%) at day 30 ($P < 0.001$). After circumlimbal suture, the RGC density decreased to 1791 ± 506 (95.0% ± 26.8%) at day 14 and 1413 ± 519 (74.9% ± 27.5%) at day 30 ($P = 0.028$) (Table 3; Figs. 4, 5A–5D).

For the SD rats, the average RGC density (cell counts/mm$^2$) was 1872 ± 210, which had decreased to 1703 ± 617 (91.0% ± 33.0%) at day 14 and 1694 ± 430 (90.5% ± 22.9%) at day 30 after magnetic bead injec-

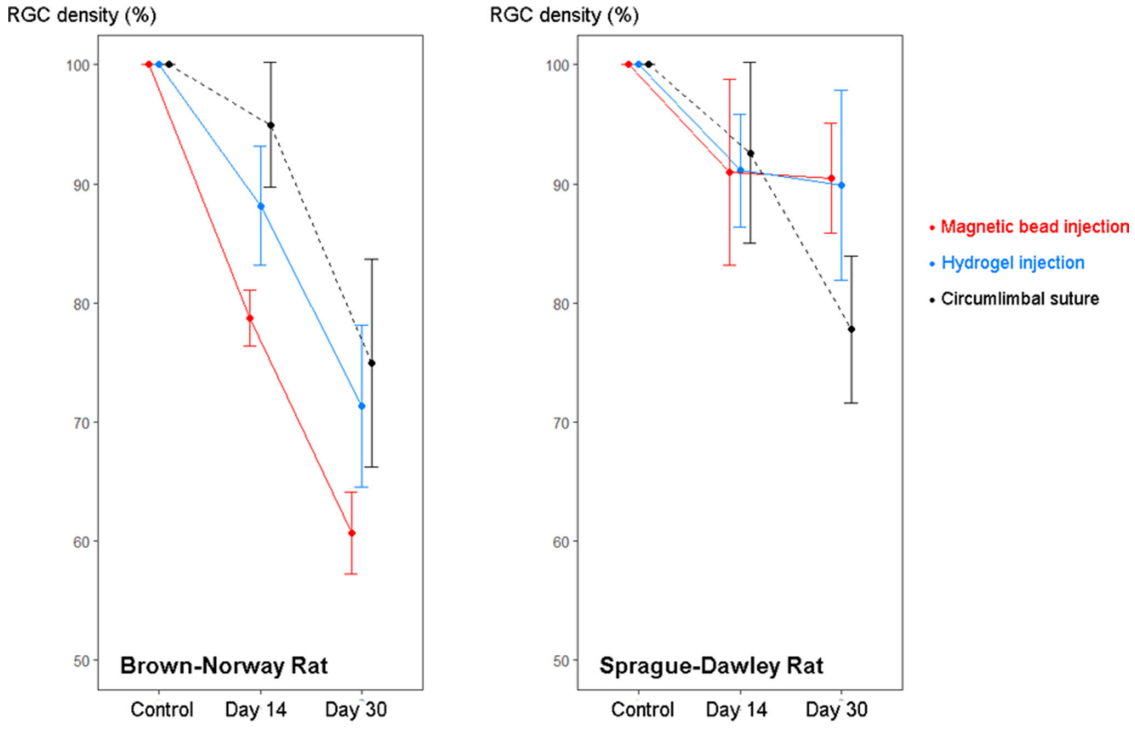


**Figure 4.** RGC density percentage changes from baseline according to strains and rodent glaucoma models. From the flat-mounted retina, a total of 36 images for each eye (three spots for each 1-, 2-, and 3-mm area from the optic nerve head in four quadrants) were obtained, and the average values were used in the analysis. In both BN and SD rats, decreases in RGC density were observed in the following order: magnetic bead injection model, hydrogel injection model, circumlimbal suture model. *Bars* indicate 95% confidence interval.

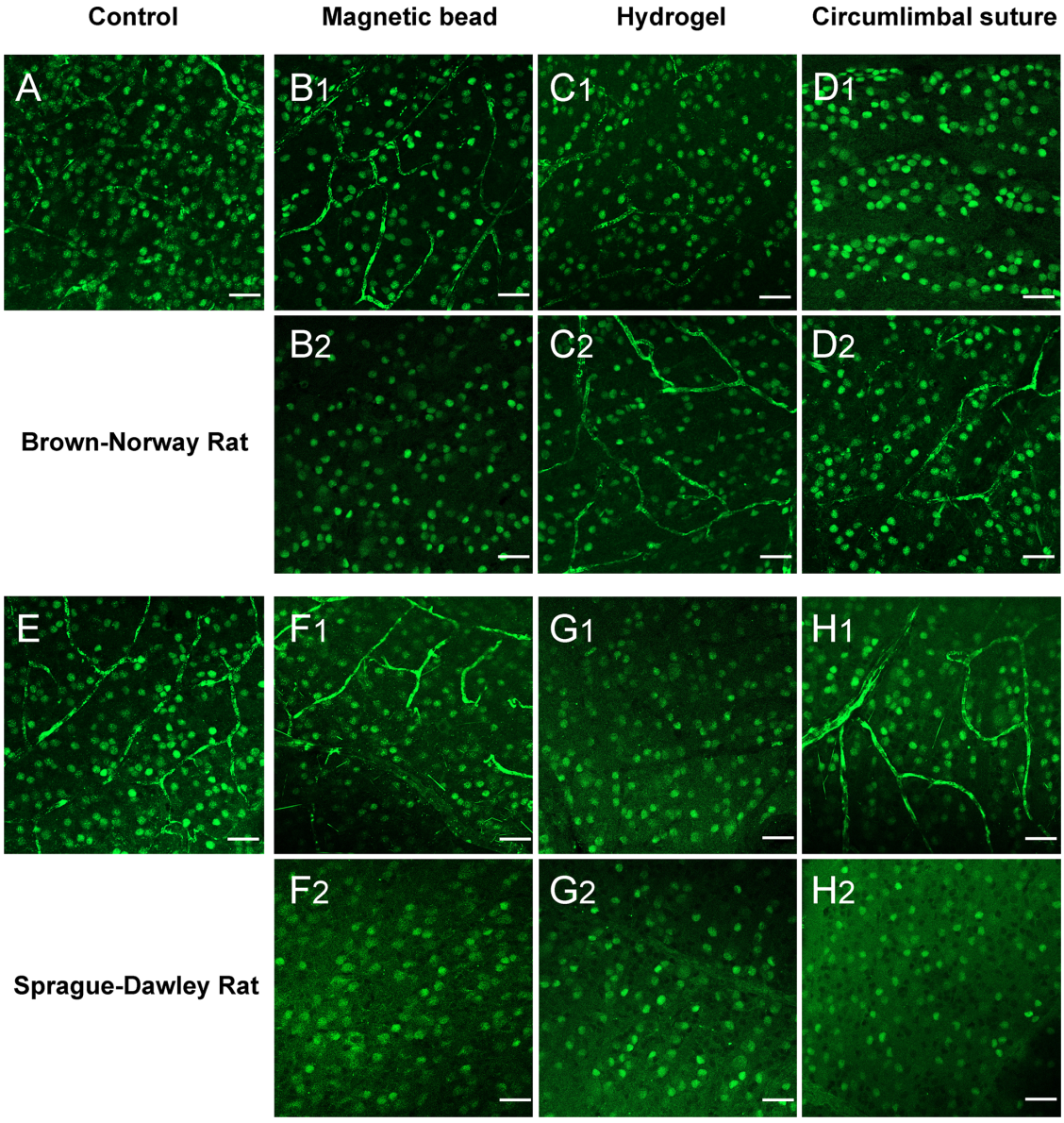


**Figure 5.** Brn3a-stained RGCs. *Scale bar*: 20 µm. (A–D) BN rats. (A) Control. (B) Magnetic bead injection model at day 14 ($B_1$) and day 30 ($B_2$). (C) Hydrogel injection model at day 14 ($C_1$) and day 30 ($C_2$). (D) Circumlimbal suture model at day 14 ($D_1$) and day 30 ($D_2$). (E–H) SD rats. (E) Control. (F) Magnetic bead injection model at day 14 ($F_1$) and day 30 ($F_2$). (G) Hydrogel injection model at day 14 ($G_1$) and day 30 ($G_2$). (H) Circumlimbal suture model at day 14 ($H_1$) and day 30 ($H_2$).

tion ($P = 0.425$). After hydrogel injection, the RGC density decreased to 1706 ± 416 (91.1% ± 22.2%) at day 14 and 1683 ± 446 (89.9% ± 23.8%) at day 30 ($P = 0.489$). After circumlimbal suture, the RGC density decreased to 1734 ± 494 (92.6% ± 26.4%) at day 14 and 1456 ± 432 (77.8% ± 23.1%) at day 30 ($P < 0.001$) (Table 3; Figs. 4, 5E–5H).

## Discussion

In this study, we compared three inducible rodent glaucoma models against two different rat strains. Ocular hypertension was induced either by internal blockage of aqueous humor outflow (with magnetic bead or hydrogel injection) or by external compression with circumlimbal suture, which is thought to render aqueous humor overflow excessive of drainage capacity.[18] With both strains, the magnetic bead injection model resulted in a steady increase of IOP without spikes, whereas the hydrogel injection model and circumlimbal suture model required an immediate IOP spike to maintain increased IOP for more than 2 weeks. For the internal approach (magnetic bead or hydrogel injection), the BN rats were superior to the SD rats with regard to maintaining increased IOP. No

such strain difference was observed for the external approach (i.e., the circumlimbal suture model). This implied that different strains might affect increases in IOP differently depending on the model mechanism and thus should be considered cautiously when establishing any rodent glaucoma model.

The use of magnetic beads has the merit of preventing reflux spillage during needle removal, specifically by means of a magnet that keeps the beads away from the needle track (Supplementary Movie S1). Upon needle removal, the high-pressure gradient between the inside and outside of the eyeball and the patent needle track leads to reflux of the aqueous humor and beads. To prevent this, we adopted three strategies: (1) use of a glass capillary needle fabricated to have very narrow and sharp tip, (2) performing an incision parallel to the corneal limbus to make a longer track, and (3) use of magnetic beads and a magnet to hold the beads at the end of procedure. In this way, we could prevent spillage of magnetic beads, although aqueous humor reflux could not be completely blocked. The magnetic bead injection model showed a steady increase of IOP without any immediate IOP spike. This absence of IOP spike might be the result of the incomplete blocking of aqueous humor reflux, which presumably neutralized IOP in the immediately postoperative period.

The magnetic bead injection model produced two gross anatomical changes. First, the steady IOP increase induced apparent buphthalmos in all BN rats and in some of the SD rats; in fact, global eyeball expansion after magnetic bead injection in BN rats has been reported.[32] As occurs in congenital glaucoma, eyeball expansion might be possible under conditions of elastic sclera and steady IOP increase.[32,44,45] Although less evident, buphthalmos also was observed in the SD rats in the present study. Its lesser occurrence in SD rats might be associated with poorer maintenance of the IOP increase with the magnetic bead injection model. As for the second gross anatomical change produced by the magnetic bead injection model, it, unlike the other two models, induced neovascular complications including iris neovascularization and hyphema, although rarely. In our pilot study, the larger magnetic bead injection volume could enable better IOP maintenance from the immediately postoperative period, but it also led to greater chances of neovascular complications. Therefore, we should limit the injected magnetic bead volume for a steady IOP increase. In contrast, no neovascular complication was observed in the hydrogel injection or circumlimbal suture models, despite much higher IOP spikes in the immediately postoperative period. Thus, we speculated, as did Tribble et al.,[32] that magnetic bead injection itself might induce vascular compromise.

In the hydrogel injection model, aqueous humor outflow was blocked by the hydrogel, which had been transformed to the gel state after its injection. Because the premixed agent was injected in the liquid state, no needle blockage by the injected particles could occur, which allowed for the use of a very fine glass needle tip. Consequently, reflux was minimized, even to the extent that enabled immediately postoperative IOP spikes. Further, the anterior segment of the eye was unaffected by the particles, due to the transparency of the gel material (Supplementary Movie S2). This certainly would be a great advantage in terms of postoperative imaging. Unfortunately, however, the IOP increase could not be maintained for more than 2 weeks without a booster injection. This was the reason for having to set a very high immediately postoperative IOP to maintain IOP elevation longer. Because eyeball expansion was rarely observed, we speculated that this model might simulate a subacute IOP elevation model better than chronic glaucoma. Insufficient IOP elevation in the hydrogel model, however, should be interpreted with caution. Our hydrogel model had less IOP elevation when compared to the reference work of Huang et al.[34] Later, Yu et al.[37] showed not only IOP elevation but also functional impairments, which were reversed after IOP-lowering treatments in the hydrogel injection model using SD rats. Therefore, our hydrogel injection method might have to be optimized further. Moreover, newer hydrogel agents[36,38,46] and post-injection modifications using ultraviolet lights[35,38] have been developed. Therefore, we speculated that the hydrogel injection model can be further improved in the future.

The circumlimbal suture model also required a very high immediately postoperative IOP. This IOP elevation had dropped by the next day but remained above the normal range for a month. IOP spikes immediately after suturing have been reported consistently for the circumlimbal suture models.[18–20] This finding contrasted with the gradual decrease or gradual increase in the hydrogel injection model or magnetic bead injection model, respectively. Interestingly, no inter-strain difference was observed in this model. Because the SD rats are less expensive than the BN type, the circumlimbal suture model would be beneficial with regard to cost relative to the other models. On the other hand, this model resulted in less RGC death, which is probably related to the poorer maintenance of increased IOP. Considering the IOP profile and the absence of eyeball expansion, we speculated that the circumlimbal suture model might simulate acute IOP elevation better than chronic glaucoma.

The internal aqueous outflow blocking approach showed inter-strain differences, as increased IOP was maintained better in the BN rats than in the SD type.

Similar differential susceptibility according to strains has been reported for mice glaucoma models aiming to obstruct the aqueous humor outflow pathway with microbeads. Cone et al.[22,26] induced an experimental glaucoma model by injecting microbeads and viscoelastics into C57/BL6, DBA/2J, and CD1 mice, and the smallest extent of IOP elevation was observed in the CD1 mice. Because both SD rats and CD1 mice have white hairs, unlike other strains, we speculated that the amount of pigmentation might affect obstruction at the level of the trabecular meshwork, as observed in pigmentary glaucoma.[47] This might in fact be one clue to ethnic differences in glaucoma manifestation.[48] Further study is necessary to confirm this speculation.

Host immunologic reaction might be another reason for the difference in susceptibility between the internal and external approaches. In contrast to the external approach, intracameral injection of foreign bodies could aggravate inflammation.[27] Further, Kezic et al.[49] showed that anterior chamber cannulation alone could induce microglial activation, whereas the concomitant IOP elevation led to additional Müller cell activation. Therefore, IOP elevation through the internal aqueous outflow blocking approach may be due in part to inflammatory trabeculitis.[10,21] Interestingly, the retinal pigment epithelium has been reported to contribute to the immune and inflammatory response of the eye not only as part of the blood–eye barrier preserving the immune-privileged status but also by being the source and target of inflammatory cytokines.[50] Thus, strains with different pigmentation status may show different immunologic reactions. Although we did not observe any gross anatomical difference in inflammation, the differences among the glaucoma models observed in this study could become a cornerstone of a novel immunologic evaluation of glaucoma pathogenesis.[4]

This study has several limitations. First, this study evaluated only RGC density as the result of elevated IOP in each glaucoma animal model. Evaluation of other retinal cells (such as bipolar cells or photoreceptors) would have been helpful in order to quantify which model led to more RGC-specific injury and thus would be more useful as a glaucoma model. Second, despite our success in demonstrating the different clinical profiles of each glaucoma animal model according to strains, we could not determine the exact reason for such differences. Further study would be required to elucidate the downstream molecular pathways of each model. Third, variation of RGC density existed among the glaucoma models. This was somewhat inevitable, as we could not control for the exact IOP status of every subject. Further, cases with neovascular complications had to be excluded from the magnetic bead injection model due to the fact that flat mounting of the retina was not possible. And, because those cases were generally associated with higher IOP, we might have excluded severe cases selectively, thus leading to underestimation of RGC deaths in our models. RGC density would be more informative if, in future work, IOP status also could be incorporated into models for comparative purposes. Fourth, our comparison of RGC density was based on cross-sectional data, not longitudinal data, because we had to sacrifice the rats in order to count RGCs on the retinal flat mounts. In vivo real-time evaluation of RGCs and their function would be necessary to elucidate the individual effect of IOP change over time in each glaucoma model in the future. Fifth and finally, we did not compare the IOP-normalizing treatment outcomes according to the models and strains. Given that the ultimate goal of these models is to develop novel human glaucoma treatment strategies, further study on the treatment outcomes of different models and strains based on the conventional treatment would be helpful.

In conclusion, the magnetic bead and hydrogel injection models were affected by animal strain but the circumlimbal suture model was not. Strains should be considered as an important factor when establishing rodent glaucoma animal models. Our recommendations are as follows: (1) use the magnetic bead injection model with BN rats if a steady increase in IOP is required, as occurs in chronic glaucoma; (2) use the hydrogel injection model with BN rats if ocular imaging is planned; and (3) use the circumlimbal suture model with either BN or SD rats if acute increases of IOP are required.

## Acknowledgments

Supported by a multidisciplinary research grant-in-aid from the Seoul Metropolitan Government–Seoul National University Boramae Medical Center (04-2022-29). The funders had no role in the study design, data collection and analysis, decision to publish, or preparation of the manuscript.

Disclosure: **K.M. Lee**, None; **D.Y. Song**, None; **S.H. Kim**, None

## References

1. Quigley HA, Broman AT. The number of people with glaucoma worldwide in 2010 and 2020. *Br J Ophthalmol*. 2006;90:262–267.
2. Tham YC, Li X, Wong TY, Quigley HA, Aung T, Cheng C-Y, et al. Global prevalence of glaucoma

and projections of glaucoma burden through 2040: a systematic review and meta-analysis. *Ophthalmology*. 2014;121:2081–2090.
3. Flaxman SR, Bourne RRA, Resnikoff S, et al. Global causes of blindness and distance vision impairment 1990–2020: a systematic review and meta-analysis. *Lancet Glob Health*. 2017;5:e1221–e1234.
4. Weinreb RN, Khaw PT. Primary open-angle glaucoma. *Lancet*. 2004;363:1711–1720.
5. Burgoyne CF. A biomechanical paradigm for axonal insult within the optic nerve head in aging and glaucoma. *Exp Eye Res*. 2011;93:120–132.
6. Quigley HA. Glaucoma. *Lancet*. 2011;377:1367–1377.
7. Weinreb RN, Aung T, Medeiros FA. The pathophysiology and treatment of glaucoma: a review. *JAMA*. 2014;311:1901–1911.
8. Quigley HA, Addicks EM. Chronic experimental glaucoma in primates. II. Effect of extended intraocular pressure elevation on optic nerve head and axonal transport. *Invest Ophthalmol Vis Sci*. 1980;19:137–152.
9. Quigley HA, Hohman RM. Laser energy levels for trabecular meshwork damage in the primate eye. *Invest Ophthalmol Vis Sci*. 1983;24:1305–1307.
10. Weber AJ, Zelenak D. Experimental glaucoma in the primate induced by latex microspheres. *J Neurosci Methods*. 2001;111:39–48.
11. Kumar S, Benavente-Perez A, Ablordeppey R, et al. A robust microbead occlusion model of glaucoma for the common marmoset. *Transl Vis Sci Technol*. 2022;11:14.
12. Samuelson DA, Gum GG, Gelatt KN. Ultrastructural changes in the aqueous outflow apparatus of beagles with inherited glaucoma. *Invest Ophthalmol Vis Sci*. 1989;30:550–561.
13. Grozdanic SD, Betts DM, Sakaguchi DS, Allbaugh RA, Kwon YH, Kardon RH. Laser-induced mouse model of chronic ocular hypertension. *Invest Ophthalmol Vis Sci*. 2003;44:4337–4346.
14. Nakazawa T, Nakazawa C, Matsubara A, et al. Tumor necrosis factor-$\alpha$ mediates oligodendrocyte death and delayed retinal ganglion cell loss in a mouse model of glaucoma. *J Neurosci*. 2006;26:12633–12641.
15. McKinnon SJ, Schlamp CL, Nickells RW. Mouse models of retinal ganglion cell death and glaucoma. *Exp Eye Res*. 2009;88:816–824.
16. Gross RL, Ji J, Chang P, et al. A mouse model of elevated intraocular pressure: retina and optic nerve findings. *Trans Am Ophthalmol Soc*. 2003;101:163–169; discussion 169–171.
17. Ruiz-Ederra J, Verkman AS. Mouse model of sustained elevation in intraocular pressure produced by episcleral vein occlusion. *Exp Eye Res*. 2006;82:879–884.
18. Liu HH, Bui BV, Nguyen CT, Kezic JM, Vingrys AJ, He Z. Chronic ocular hypertension induced by circumlimbal suture in rats. *Invest Ophthalmol Vis Sci*. 2015;56:2811–2820.
19. Zhao D, Nguyen CT, Wong VH, et al. Characterization of the circumlimbal suture model of chronic IOP elevation in mice and assessment of changes in gene expression of stretch sensitive channels. *Front Neurosci*. 2017;11:41.
20. Lee SH, Sim KS, Kim CY, Park TK. Transduction pattern of AAVs in the trabecular meshwork and anterior-segment structures in a rat model of ocular hypertension. *Mol Ther Methods Clin Dev*. 2019;14:197–205.
21. Urcola JH, Hernandez M, Vecino E. Three experimental glaucoma models in rats: comparison of the effects of intraocular pressure elevation on retinal ganglion cell size and death. *Exp Eye Res*. 2006;83:429–437.
22. Cone FE, Gelman SE, Son JL, et al. Differential susceptibility to experimental glaucoma among 3 mouse strains using bead and viscoelastic injection. *Exp Eye Res*. 2010;91:415–424.
23. Sappington RM, Carlson BJ, Crish SD, Calkins DJ. The microbead occlusion model: a paradigm for induced ocular hypertension in rats and mice. *Invest Ophthalmol Vis Sci*. 2010;51:207–216.
24. Chen H, Wei X, Cho KS, et al. Optic neuropathy due to microbead-induced elevated intraocular pressure in the mouse. *Invest Ophthalmol Vis Sci*. 2011;52:36–44.
25. Samsel PA, Kisiswa L, Erichsen JT, Cross SD, Morgan JE. A novel method for the induction of experimental glaucoma using magnetic microspheres. *Invest Ophthalmol Vis Sci*. 2011;52:1671–1675.
26. Cone FE, Steinhart MR, Oglesby EN, Kalesnykas G, Pease ME, Quigley HA. The effects of anesthesia, mouse strain and age on intraocular pressure and an improved murine model of experimental glaucoma. *Exp Eye Res*. 2012;99:27–35.
27. Rho S, Park I, Seong GJ, et al. Chronic ocular hypertensive rat model using microbead injection: comparison of polyurethane, polymethylmethacrylate, silica and polystyrene microbeads. *Curr Eye Res*. 2014;39:917–927.
28. Morgan JE, Tribble JR. Microbead models in glaucoma. *Exp Eye Res*. 2015;141:9–14.
29. Ito YA, Belforte N, Cueva Vargas JL, Di Polo AA. Magnetic microbead occlusion model to induce

ocular hypertension-dependent glaucoma in mice. *J Vis Exp*. 2016;109:e53731.

30. Biswas S, Wan KH. Review of rodent hypertensive glaucoma models. *Acta Ophthalmol*. 2019;97:e331–e340.
31. Calkins DJ, Lambert WS, Formichella CR, McLaughlin WM, Sappington RM. The microbead occlusion model of ocular hypertension in mice. *Methods Mol Biol*. 2018;1695:23–39.
32. Tribble JR, Otmani A, Kokkali E, Lardner E, Morgan JE, Williams PA. Retinal ganglion cell degeneration in a rat magnetic bead model of ocular hypertensive glaucoma. *Transl Vis Sci Technol*. 2021;10:21–21.
33. Chen J, Sun J, Yu H, Huang P, Zhong Y. Evaluation of the effectiveness of a chronic ocular hypertension mouse model induced by intracameral injection of cross-linking hydrogel. *Front Med (Lausanne)*. 2021;8:643402.
34. Huang S, Huang P, Liu X, et al. Relevant variations and neuroprotective effect of hydrogen sulfide in a rat glaucoma model. *Neuroscience*. 2017;341:27–41.
35. Guo C, Qu X, Rangaswamy N, et al. A murine glaucoma model induced by rapid in vivo photopolymerization of hyaluronic acid glycidyl methacrylate. *PLoS One*. 2018;13:e0196529.
36. Chan KC, Yu Y, Ng SH, et al. Intracameral injection of a chemically cross-linked hydrogel to study chronic neurodegeneration in glaucoma. *Acta Biomater*. 2019;94:219–231.
37. Yu H, Zhong H, Chen J, et al. Efficacy, drug sensitivity, and safety of a chronic ocular hypertension rat model established using a single intracameral injection of hydrogel into the anterior chamber. *Med Sci Monit*. 2020;26:e925852.
38. Kim YK, Kim SN, Min CH, et al. Novel glaucoma model in rats using photo-crosslinked azidobenzoic acid-modified chitosan. *Mater Sci Eng C Mater Biol Appl*. 2021;125:112112.
39. Wang W-H, Millar JC, Pang I-H, Wax MB, Clark AF. Noninvasive measurement of rodent intraocular pressure with a rebound tonometer. *Invest Ophthalmol Vis Sci*. 2005;46:4617–4621.
40. Chauhan BC, Pan J, Archibald ML, LeVatte TL, Kelly MEM, Tremblay F. Effect of intraocular pressure on optic disc topography, electroretinography, and axonal loss in a chronic pressure-induced rat model of optic nerve damage. *Invest Ophthalmol Vis Sci*. 2002;43:2969–2976.
41. Cone FE, Steinhart MR, Oglesby EN, Kalesnykas G, Pease ME, Quigley HA. The effects of anesthesia, mouse strain and age on intraocular pressure and an improved murine model of experimental glaucoma. *Exp Eye Res*. 2012;99:27–35.
42. Frankfort BJ, Khan AK, Tse DY, et al. Elevated intraocular pressure causes inner retinal dysfunction before cell loss in a mouse model of experimental glaucoma. *Invest Ophthalmol Vis Sci*. 2013;54:762–770.
43. Guymer C, Damp L, Chidlow G, Wood J, Tang YF, Casson R. Software for quantifying and batch processing images of Brn3a and RBPMS immunolabelled retinal ganglion cells in retinal whole-mounts. *Transl Vis Sci Technol*. 2020;9:28.
44. Terraciano AJ, Sidoti PA. Management of refractory glaucoma in childhood. *Curr Opin Ophthalmol*. 2002;13:97–102.
45. Stowell C, Burgoyne CF, Tamm ER, Ethier CR. Biomechanical aspects of axonal damage in glaucoma: a brief review. *Exp Eye Res*. 2017;157:13–19.
46. Liu Y, Wang J, Jin X, et al. A novel rat model of ocular hypertension by a single intracameral injection of cross-linked hyaluronic acid hydrogel (Healaflow®). *Basic Clin Pharmacol Toxicol*. 2020;127:361–370.
47. Okafor K, Vinod K, Gedde SJ. Update on pigment dispersion syndrome and pigmentary glaucoma. *Curr Opin Ophthalmol*. 2017;28:154–160.
48. Gracitelli CPB, Zangwill LM, Diniz-Filho A, et al. Detection of glaucoma progression in individuals of African descent compared with those of European descent. *JAMA Ophthalmol*. 2018;136:329–335.
49. Kezic JM, Chrysostomou V, Trounce IA, et al. Effect of anterior chamber cannulation and acute IOP elevation on retinal macrophages in the adult mouse. *Invest Ophthalmol Vis Sci*. 2013;54:3028–3036.
50. Holtkamp GM, Kijlstra A, Peek R, de Vos AF. Retinal pigment epithelium–immune system interactions: cytokine production and cytokine-induced changes. *Prog Retin Eye Res*. 2001;20:29–48.

## Supplementary Material

Supplementary Movie S1. Magnetic bead injection model.

Supplementary Movie S2. Hydrogel injection model.

Supplementary Movie S3. Circumlimbal suture model.